Subsurface Patterning and its Effect on Interfacial Adhesion

Edwin P. Chan and Christopher M. Stafford
Polymers Division, National Institute of Standards and Technology, Gaithersburg, MD, USA
chris.stafford@nist.gov

Introduction

Nature (e.g. geckos and insects) has illustrated that a patterned surface can effectively tailor the adhesion of an interface.[1] Inspired by the amazing attachment and detachment ability of these animals, significant efforts have been put forth to understand the effects of patterned surfaces on polymer adhesion.[2-10] While patterned surfaces have been demonstrated to tailor and even enhance polymer adhesion, the adhesion of a flat interface that consists of subsurface patterns remains largely unexplored.[11] Compared with surface patterns, a subsurface pattern is particularly interesting since it provides a practical means to dynamically change adhesion without directly altering the interfacial properties. For example, this approach will be especially useful as a responsive adhesive that can provide on-demand release.

In this presentation, we investigate the role of subsurface patterns in controlling the adhesion of a flat interface consisting of a poly(dimethylsiloxane) (PDMS) elastomer and an inorganic surface. The subsurface pattern consists of a wrinkled interface that is buried within the PDMS elastomer. A cantilever-based peel test is used to measure the adhesion of these subsurface patterned elastomers. We explore the effects of wrinkle pattern dimensions in controlling the adhesion of these materials.

Experimental†

The subsurface patterned adhesive is a bilayered polymer film consisting of a rigid, wrinkled bottom layer and a soft, elastomeric top layer (Fig. 1). The bottom layer consists of a photocured Norland Optical Adhesive (NOA 81, Norland Products, Inc.) that is patterned with a wrinkle structure.

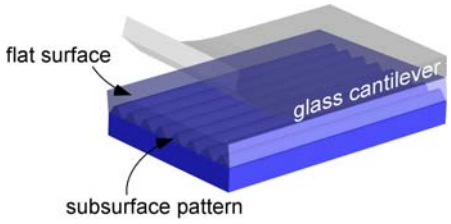

Figure 1. A subsurface pattern consisting of rigid wrinkles of NOA buried beneath the smooth, non-patterned PDMS layer.

The patterning process begins with preparing a wrinkled template fabricated by oxidizing a uniaxially stretched PDMS elastomer with ultra-violet/ozone (UVO).[12, 13] Next, the NOA is spin-coated onto a silicon substrate and then the template is placed over the liquid adhesive to replicate the wrinkle pattern. The assembly is then irradiated by UV (EFOS Acticure A4000, max. intensity ≈20 mW/cm^2) for ~5 min, which photocures the NOA 81 to form an optically transparent, rigid patterned layer. This wrinkled surface is then coated with uncured PDMS (Sylgard 184, Dow Corning Corp.). A silanized glass cantilever is placed over the uncured PDMS layer and the entire assembly is then thermally cured to form the subsurface patterned adhesive.

Following fabrication of the materials, we quantify their adhesion using a custom-built cantilever peel adhesion test (CPAT) instrument (Fig. 2). Briefly, the test measures adhesion between the glass cantilever and the smooth PDMS surface by vertically deflecting the cantilever at a fixed displacement rate (≈5 μm/s) controlled by a nanopositioner stepper motor. The force (P), vertical displacement (δ), and crack propagation length (a) are monitored throughout the course of the test.

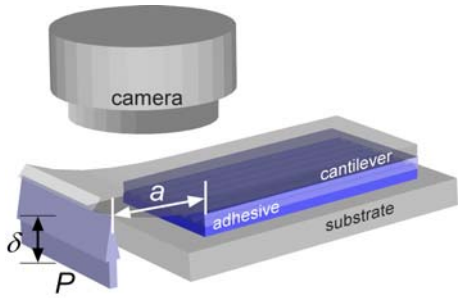

Figure 2. Cantilever peel adhesion testing of the polymer adhesive. The test measures the adhesion between the glass cantilever-smooth PDMS interface.

Results and Discussion

Representative force-displacement of a CPAT test is presented in Fig. 3. In the initial stage of the test, all the energy is applied to the deflection of the cantilever and the elastic deformation of the adhesive layer. At a critical deflection, sufficient energy is applied to cause separation of the interface. As a result, the separation process begins with the initiation of the crack and an increase in a. As the crack continues to propagate, both a and δ continue to increase.

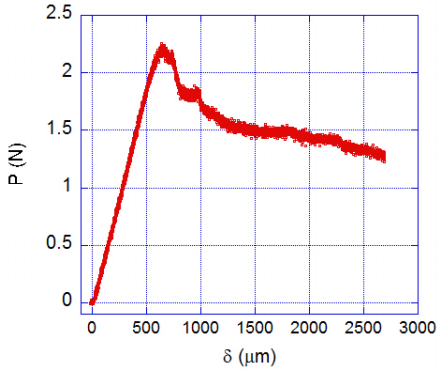

Figure 3. Representative force-displacement (P-δ) curve for the cantilever peel adhesion testing of the polymer adhesive.

The critical energy release rate (G_c) of the interface can be quantified using the experimentally-measured quantities of flexural stiffness (D), displacement (δ) and crack length (a). For films that are semi-infinite in thickness, G_c can be estimated with the classical Obreimoff equation (Eqn. 1).[14]

$$G_c = \frac{9}{2} D \frac{\delta^2}{a^4} \qquad (1)$$

For the thickness of the adhesives explored (≈100 μm ± 20 μm), the separation occurred through the development of an interfacial instability at the glass-PDMS interface (Fig. 4a). These elastic instabilities, whose wavelength (λ_i) scales with the thickness of the PDMS layer, have been previously observed by Ghatak and coworkers, and are associated with relief of stress at the crack front.[15, 16]

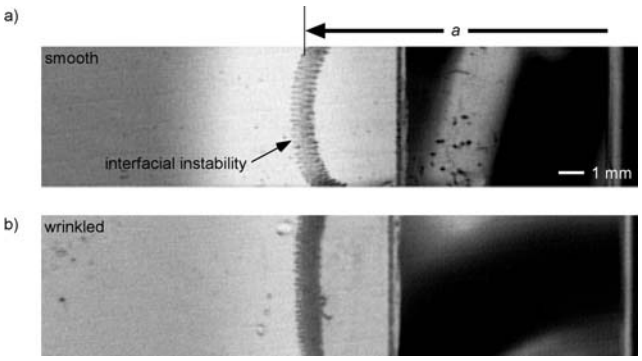

Figure 4. Cantilever peel adhesion testing of the polymer adhesive.

We expect that the changes in G_c of our materials will be a function of the commensurability between the wavelength of the interfacial instability (λ_i) and the wavelength of the subsurface wrinkle pattern (λ_e). Since λ_i is related to the thickness of the adhesive layer, λ_e will affect the development of the most favorable λ_i since the subsurface patterning leads to a periodic variation in film thickness.

As an example, we demonstrate the changes in the separation process as a result of the subsurface wrinkling process in Fig. 4. Similar to the smooth, non-patterned subsurface case (Fig. 4a), the presence of the subsurface wrinkles again leads to the development of the interfacial instabilities (Fig. 4b). An interesting result of the subsurface wrinkling process is the change in wavelength of the interfacial instability. Specifically, we observe that the presence of the subsurface wrinkles leads to a decrease in the wavelength of the interfacial instabilities (from $\lambda_i \approx 204$ μm ± 20 μm to $\lambda_i \approx 101$ μm ± 10 μm, with $\lambda_e \approx 172$ μm ± 20 μm). Additionally, we find that subsurface wrinkling leads to an increase in G_c. For this example, we find that the G_c is enhanced by ≈50% ± 10% relative to the smooth system. We speculate that this enhancement is related to the local change in compliance of the material (due to changes in film thickness), which leads to the subsequent local modulation of crack propagation rate.

In this contribution, we explore the commensurability in the wrinkle pattern wavelength with the material's defined adhesion-induced instability wavelength by investigating the influence of the distance of subsurface wrinkles on the adhesion of smooth PDMS surface. Specifically, we measure the adhesion of our materials as a function of the thickness of the PDMS layer (h_{PDMS}) while maintaining a constant wrinkle wavelength, amplitude, and orientation.

Acknowledgements

The authors thank Dr. Jun Young Chung for experimental assistance and helpful discussions.

† Equipment and instruments or materials are identified in this work in order to adequately specify the experimental details. Such identification does not imply recommendation by the National Institute of Standards and Technology (NIST), nor does it imply that the materials are necessarily the best available for the purpose.

References

[1] S. N. Gorb, *Attachment devices of insect cuticle*, Kluwer Academic Publishers, Dordrecht, **2001**.

[2] A. K. Geim, S. V. Dubonos, I. V. Grigorieva, K. S. Novoselov, A. A. Zhukov, S. Y. Shapoval, *Nat. Mater.* **2003**, *2*, 461.

[3] N. J. Glassmaker, A. Jagota, C.-Y. Hui, J. Kim, *J. R. Soc. Interface* **2004**, *1*, 23.

[4] C. Y. Hui, N. J. Glassmaker, T. Tang, A. Jagota, *J. R. Soc. Interface* **2004**, *1*, 35.

[5] A. J. Crosby, M. Hageman, A. Duncan, *Langmuir* **2005**, *21*, 11738.

[6] S. Kim, M. Sitti, *Appl. Phys. Lett.* **2006**, *89*.

[7] B. Aksak, M. P. Murphy, M. Sitti, *Langmuir* **2007**, *23*, 3322.
[8] C. Greiner, A. del Campo, E. Arzt, *Langmuir* **2007**, *23*, 3995.
[9] M. Lamblet, E. Verneuil, T. Vilmin, A. Buguin, P. Silberzan, L. Leger, *Langmuir* **2007**, *23*, 6966.
[10] S. J. Kwon, J.-H. Park, J. G. Park, *Phys. Rev. E* **2005**, *71*, 011604.
[11] A. Majumder, A. Ghatak, A. Sharma, *Science* **2007**, *318*, 258.
[12] N. Bowden, W. T. S. Huck, K. E. Paul, G. W. Whitesides, *Applied Physics Letters* **1999**, *75*, 2557.
[13] K. Efimenko, M. Rackaitis, E. Manias, A. Vaziri, L. Mahadevan, J. Genzer, *Nature Materials* **2005**, *4*, 293.
[14] J. W. Obreimoff, *Proc. R. Soc. London, Ser. A* **1930**, *127*, 290.
[15] A. Ghatak, M. K. Chaudhury, V. Shenoy, A. Sharma, *Physical Review Letters* **2000**, *85*, 4329.
[16] A. Ghatak, L. Mahadevan, M. K. Chaudhury, *Langmuir* **2005**, *21*, 1277.